Ecological Indicators 178 (2025) 114126

Contents lists available at ScienceDirect

Ecological Indicators

journal homepage: www.elsevier.com/locate/ecolind

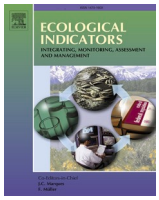

Original Articles

# Multiple methods reveal the carbon stock potential of young reforested mangroves in Quanzhou Bay Nature Reserve, China

Yi-Jia Shih [a,b], Kai Liu [a,*], Shu-Chiang Huang [c], Yi Chang [c,d], Fen-Fen Ji [a], Chun-Xi Cao [e], Mou-Xin Ye [e], Yi-Min Li [f], Yi-Hua Jin [g], You-Rong Yao [h]

[a] Fisheries College, Jimei University, Xiamen 361021, China
[b] Sustainable Ocean Governance Centre, National Sun Yat-sen University, Kaohsiung 80424, Taiwan
[c] Graduate Institute of Marine Affairs, National Sun Yat-sen University, Kaohsiung 80424, Taiwan
[d] Center for Carbon Research and Solutions, National Sun Yat-sen University, Kaohsiung 80424, Taiwan
[e] Mangrove Conservation Foundation (MCF), Shenzhen 518000, China
[f] Administrative Office of Quanzhou Bay Estuary Wetland Nature Reserve, Quanzhou 362121, China
[g] Department of Marine Environment and Engineering, National Sun Yat-sen University, Kaohsiung 80421, Taiwan
[h] Faculty of Social Sciences, University of Macau, Macau, China

ARTICLE INFO

*Keywords:*
Mangrove reforestation
Mixed plantation
Mangrove young stage
Carbon stock
Quanzhou Bay

ABSTRACT

Mangrove reforestation has emerged as a critical component in blue carbon, with its carbon sequestration potential receiving increasing attention. However, most existing studies have focused on mature mangrove stands and adopted generalized assessment approaches, often ignoring the dynamics of plant growth, thereby raising concerns about the accuracy and reliability of carbon sequestration estimations. In this study, a site-based was assessed in a juvenile mangrove reforestation experimental area within the Quanzhou Bay Estuarine Wetland Natural Reserve from December 2022 to 2024, using three complementary models to evaluate early-stage carbon accumulation. Model I applied species-specific allometric equations suitable for saplings (basal diameter $< 4$ cm); Model II employed general equations commonly used for estimating biomass in more mature stands (DBH $\geq 4$ cm); and Model III assessed vegetative expansion using NDVI-based remote sensing. The results revealed the cumulative carbon stock ranging from 45.34 to 158.84 t C, corresponding to a $CO_2$ sequestration potential of 166.25 to 582.41 t $CO_2$. Moreover, based on biomass increments, annual carbon sequestration rates were calculated for five species and two reforestation strategies (mixed vs. monoculture forests). Under Model I, sequestration rates increased from 9.58 to 24.74 t C $yr^{-1}$ in mixed forests and from 3.73 to 7.52 t C $yr^{-1}$ in monocultures. Model II produced consistently higher estimates, with mixed forests rising from 8.96 to 27.23 t C $yr^{-1}$ and monocultures from 28.38 to 35.18 t C $yr^{-1}$. These trends highlight accelerated carbon accumulation during the second year and variation between models and planting strategies. Cumulative carbon stocks increased significantly in the second year, and *Kandelia obovata* contributed the highest species-level carbon stock. Statistical analysis also showed that mixed forests (Area A) consistently outperformed monocultures forests (Area B) in biomass accumulation ($p$-value $< 0.0001$), but NDVI failed to reflect these differences. The result was highlighting its limitations in detecting early-stage structural complexity. These findings suggest that Model I is more appropriate for evaluating biomass accumulation during the juvenile phase, and that reliance on NDVI alone may underestimate early-stage carbon stock. Overall, a phased evaluation was proposed that integrates multiple methodologies to enhance the accuracy of mangrove carbon sequestration assessments in this study. This approach holds promise for improving the scientific basis of carbon offset verification and informing risk assessment in blue carbon trading schemes.

* Corresponding author.
*E-mail address:* liukai1218@jmu.edu.cn (K. Liu).

https://doi.org/10.1016/j.ecolind.2025.114126
Received 27 March 2025; Received in revised form 18 August 2025; Accepted 24 August 2025
Available online 28 August 2025

## 1. Introduction

Climate change is driven by a combination of anthropogenic activities and natural environmental variability. Among these, the rise in greenhouse gas (GHG) concentrations have become one of the most critical concerns. Numerous studies have shown that the rapid increase in GHG level has intensified global climate instability and increase the frequency of extreme weather events and altered species distributions (Pecl et al., 2017). These environmental changes pose significant challenges to both natural ecosystems and human societies (Mora et al., 2018). In response, international agreements such as the United Nations Framework Convention on Climate Change (UNFCCC) and the Paris Agreement have been established to mitigate the risks associated with uncontrolled GHG emissions (Warren et al., 2018). To achieve carbon neutrality, countries have formulated Nationally Determined Contributions (NDCs) and adopted carbon capture and storage (CCS) technologies to reduce the environmental impact of carbon emissions (Shen et al., 2022). However, given the strong linkage between carbon emissions and economic development, relying solely on industrial emission reductions may not suffice for long-term sustainability (Mardani et al., 2019). As a result, nature-based solutions (NbS) have gained recognition as a critical strategy for enhancing carbon fixation and storage capacity (Keith et al., 2021).

NbS has demonstrated potential in the global voluntary carbon market, not only by improving CCS efficiency but also by generating economic benefits and supporting ecosystem conservation (Macreadie et al., 2019). The primary natural carbon storage mechanisms include terrestrial forests (green carbon) and coastal ecosystems (blue carbon), both of which play significant roles in CCS. While green carbon research and applications have advanced earlier, its long-term sequestration potential is limited due to aerobic microbial decomposition in terrestrial soils (Su et al., 2024). In contrast, blue carbon ecosystems, such as mangroves, salt marshes, and seagrass meadows, exhibit higher carbon stock potential due to their predominantly anaerobic sedimentary environments, which slow down carbon decomposition (Choudhary et al., 2024; Macreadie et al., 2021; Wang et al., 2023). Moreover, blue carbon ecosystems contribute to biodiversity maintenance and habitat stability, further enhancing their role in climate change mitigation and ecological adaptation (Hilmi et al., 2021).

Among blue carbon ecosystems, mangrove forests have attracted global attention due to their high carbon storage capacity and multifunctional ecosystem services; they offered well fix and store ability of carbon (24 Tg C $y^{-1}$) with high productivity (Alongi, 2014; Ruan et al., 2022). Extensive research has highlighted the significance of mangrove carbon stock in offsetting anthropogenic $CO_2$ emissions (Mcleod et al., 2011; Siikamäki et al., 2012). The growing recognition of mangroves in the carbon market has led to notable developments, such as the Vida Manglar Project in Colombia (López-Angarita et al., 2016) and the Shenzhen Mangrove Carbon Credit Initiative in China (Li et al., 2024), demonstrating the increasing potential of mangroves in blue carbon trading. The primary mechanism for mangrove carbon credit generation lies in restoration efforts, categorized into reforestation (restoring degraded mangrove habitats) and afforestation (establishing mangroves in previously non-mangrove areas) (Song et al., 2023). However, studies suggest that reforestation and afforestation may differ in carbon stock efficiency and ecosystem benefits, as reforestation occurs in historically degraded habitats where prior land-use trajectories support natural ecosystem adaptation, promoting vegetation succession dynamics and carbon flux efficiency (Estrada-Villegas et al., 2020; Hong et al., 2020; Trujillo et al., 2021). A global study on mangrove afforestation and reforestation indicates that long-term carbon storage in reforested mangroves is approximately 60 % higher than in afforested sites (Song et al., 2023).

Despite the promising carbon sink potential of mangrove reforestation, significant uncertainties remain in carbon accounting methodologies. As a result, carbon stock assessment has become a frontier research field in recent years, particularly in regions undergoing farmland-to-forest conversions and preparing to participate in voluntary carbon markets (VCM) (Battocletti et al., 2024; Christiansen, 2024; Li et al., 2024). Accurate estimation of mangrove carbon stocks requires a comprehensive assessment, including aboveground biomass (AGB), belowground biomass (BGB), and soil carbon storage, as more than 50 % of mangrove carbon is stored in belowground root systems and sediments (Alongi, 2012; Donato et al., 2011). Current methods for mangrove carbon stock assessment include: Field measurements; Remote sensing and GIS analysis; Carbon sink modeling, and Isotope and biogeochemical analysis; and the application of allometric growth models for biomass estimation and carbon stock conversion (Hamilton and Casey, 2016; Kauffman and Cole, 2010). Among these, allometric models have gained international acceptance due to their non-destructive nature and operational efficiency, and are now widely used in regional and global assessments. Nonetheless, international organizations continue to emphasize the need for more standardized and scalable frameworks to improve the consistency and accuracy of carbon sink evaluations (Mcleod et al., 2011). This is especially important given the potential for methodological discrepancies, mangrove stands, and rapid changes in forest productivity to introduce significant uncertainties in regional carbon stock estimations (Worthington et al., 2024).

In addition, the temporal dynamics of mangrove growth remain underexplored. Although young mangrove forests (<5 years or basal diameter <4 cm) generally exhibit lower biomass accumulation and limited commercial utilization potential compared to mature stands, they often display faster growth rates and higher stem densities during early successional stage (Bosire et al., 2008). These juvenile trees play a crucial role in shaping stand structure and accelerating forest development, thereby contributing substantially to ecosystem functionality. Moreover, studies have shown that young mangrove forests substantially enhance soil organic carbon concentration, highlighting their pivotal role in carbon stock dynamics (Lunstrum and Chen, 2014). Therefore, it is essential to evaluate carbon stock capacity from the early developmental stages of mangrove trees to enhance the accuracy of predictive assessments.

Southern China hosts one of the most extensive mangrove distributions in Asia, with Fujian Province historically supporting vast coastal mangrove forests. Historical records indicate that native mangrove species in this region included *Aegiceras corniculatum*, *Avicennia marina*, *Bruguiera gymnorrhiza*, *Kandelia obovata*, and *Rhizophora stylosa*. Notably, this region marks the northernmost natural distribution limits of *A. marina* and *A. corniculatum* along the western Pacific coastline (Chen et al., 2017). However, rapid economic expansion since the 1960s has resulted in severe habitat degradation due to extensive agricultural and aquaculture land development (Liu et al., 2010). In response to these challenges, the Fujian Provincial Government implemented a regulation on the management of aquaculture in coastal areas in 2000, designating specific aquaculture zones and promoting sustainable development. Despite these efforts, disturbed mudflat habitats have facilitated the large-scale invasion of *Spartina alterniflora*, significantly impacting carbon storage capacity and biodiversity (An et al., 2007; Huang et al., 2022). To mitigate these adverse effects, a large-scale *S. alterniflora* removal initiative was launched in 2024. While this initiative plays a crucial role in wetland conservation, it also presents a management challenge – ensuring ecosystem functionality is restored and reinvasion is prevented (Tang et al., 2021). Consequently, preventing the re-invasion of exposed mudflats by *S. alterniflora* while maintaining stable ecosystem service functions has become a critical management priority. In this context, mangrove restoration and reforestation offer a Nbs approach for anti-invasion of *S. alterniflora*, as well as serving a dual strategy to enhance carbon stock capacity and promote ecosystem recovery (Alongi, 2012; Van Hespen et al., 2023).

In summary, this study aims to enhance the understanding of carbon stock potential in young reforested mangrove stands by assessing early-

stage carbon storage dynamics in the Quanzhou Bay Estuarine Wetland Natural Reserve, Fujian Province. A comprehensive evaluation will be conducted to quantify carbon stock dynamics based on tree biomass contributions. To achieve this objective, a combination of tree biomass estimation and remote sensing monitoring will be employed to improve accuracy and spatial coverage. The findings of this study will establish baseline data for mangrove restoration efforts and contribute to the scientific framework for ecological restoration and biodiversity conservation, aligning with China's 'Dual Carbon' strategy.

## 2. Materials and methods

### 2.1. Study area, and planting strategy

The reforestation site was located in Fengyu Village, Fengze District, Quanzhou Bay, Fujian Province (24.9213°N, 118.6697°E), with a total planting area of 13.38 ha. This area is part of the Quanzhou Bay Estuarine Wetland Natural Reserve and is situated at the estuary of the Luojiang River, a major river flowing through Quanzhou City. Therefore, the native species and their adapted ability was be considered. The reforestation area was divided into two distinct zones (Areas A and B). Area A was planned as a mixed-species forests (*A. corniculatum, B. gymnorrhiza, K. obovata, and Rhizophora stylosa*), whereas Area B, located closer to the waterfront with higher soil salinity, was planned for a monoculture forests (*A. marina*) of salt-tolerant species. Detailed information, including location, planting ranges, planted strategy, and areas, was presented in Fig. 1.

### 2.2. Sample collection, period and estimated the plant abundance

Monitoring sites were indicated as red dots in Fig. 1, and their detailed geographic coordinates were also provided. Sampling periods were conducted in December 2022, December 2023, and December 2024. The sampling dates were scheduled to coincide with the highest monthly tidal amplitude to ensure full exposure of intertidal zone (Alongi, 2012; Kauffman and Donato, 2012; Komiyama et al., 2008). This timing ensured that Area B, including the lowest site, was fully exposed and accessible during low tide. The first monitoring event was performed in December 2022 following mangrove sapling planting. During this initial survey, a total of six permanent 3 m × 3 m monitoring sites were established across the reforested site based on the stratified sampling approach, which four in Area A and two in Area B. All sites were marked using plastic pipes. Each site was spaced at least 50 m apart from neighboring site. All mangrove individuals within each site were individually measured and anti-water tape labeled to allow consistent monitoring of marked individuals in subsequent surveys, facilitating analysis of their survival rates. These sites served dual functions – as fixed monitoring site for survival tracking and as sampling sites for biomass and carbon stock estimation. The size was considered sufficient due to the following factors: (1) The 13-hectare mangrove restoration area was uniformly planted with known species composition and consistent density. Environmentally, both Area A and B also followed the same tidal rhythm, with the intertidal zone fully exposed during low tide, resulting in broadly equivalent water coverage times and thereby minimizing spatial heterogeneity. (2) Sites were evenly distributed across both mixed and monoculture forests zones to capture variation in stand structure and species proportions. (3) The monitoring since planting has confirmed minimal tree mortality and stable growth conditions within and outside the plots. Given these controlled conditions, the selected plot size adequately represents the structural characteristics of the plantation.

Measurement protocols followed standardized methodologies outlined in the Mangrove Ecological Restoration Handbook by China (Liu and Ma, 2024). Measured parameters included basal diameter (cm), which refered to the stem diameter measured at approximately 5 cm above ground level, and tree height (m). Individual measurements of each individual (species, height, and basal diameter) were systematically recorded and digitally archived. Subsequently, species-specific planting density (individual / per hectare) was calculated and multiplied by the actual planted area to estimate the total population size of each species within the study area. The relevant calculation formulas are provided as follows:

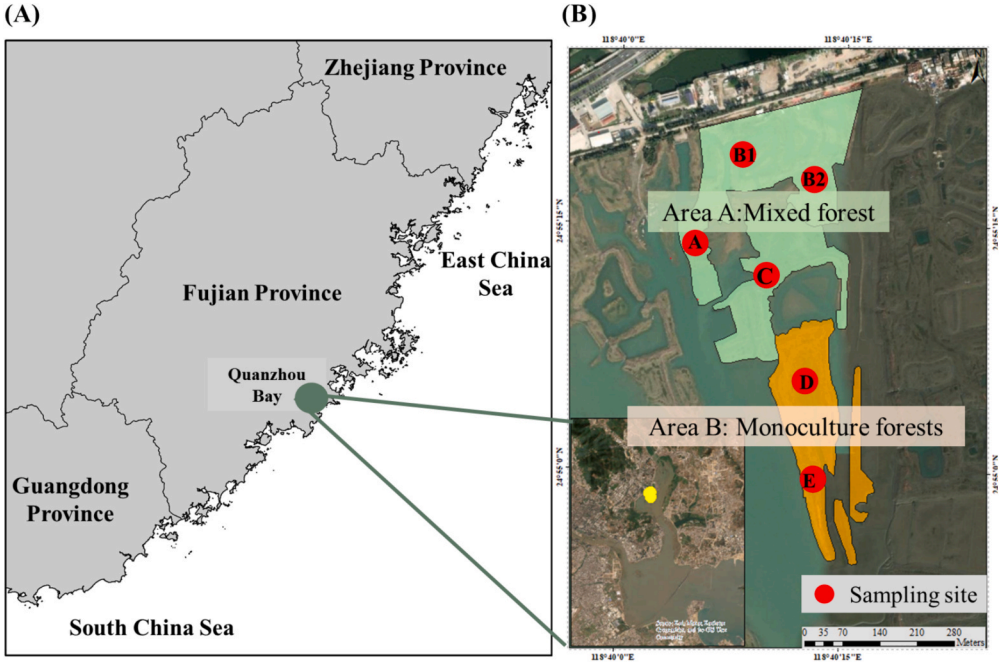


**Fig. 1.** Location of the study area and distribution of sampling sites within the Quanzhou Bay Estuarine Wetland Natural Reserve, Fujian Province, China. (A) Geographic location of Quanzhou Bay on the southeast coast of China. (B) Satellite map showing reforested mangrove zones. Light green represents Area A (mixed forests), and orange represents Area B (monoculture forests). Total six permanent sampling sites (red circles labeled) were established: four in Area A and two in Area B.

$$\text{Estimated Surviving Planted Individuals (ind.)} = \frac{\text{Surveying the number of individual (ind.)}}{\text{Sampling site area (ha)}} \times \text{Planting area (ha)}$$

### 2.3. Estimation of carbon stock based on species-specific allometric equations

Biomass estimation of mangroves, usually achieved through the application of allometric growth equations, serves as an essential approach for quantifying carbon stock potential (Perera et al., 2011). In this study, two distinct allometric equations were employed to estimate and compare biomass: Model I, derived from equations established for mangrove saplings across various sites in China. Model II, utilizing species-specific biomass equations. Detailed information regarding the equations used in each model is presented in Table S1.

Subsequently, individual biomass measurements were conducted for sampled specimens to calculate both aboveground and belowground biomass, from which mean individual biomass values were determined. These values were then used to estimate the total biomass. The calculation formula applied is as follows:

$$\text{Species Biomass}_{\text{AGB, T}}\,(\text{kg}) = \text{AGB}_{\text{single, average(kg)}} \times \text{Individuals}$$

$$\text{Species Biomass}_{\text{BGB, T}}\,(\text{kg}) = \text{BGB}_{\text{single, average(kg)}} \times \text{Individuals}$$

where,

Species Biomass $_{\text{AGB, T}}$ (kg): Total aboveground biomass of an individual species within the study area;

Species Biomass $_{\text{BGB, T}}$ (kg): Total belowground biomass of an individual species within the study area;

AGB $_{\text{single,average}}$ (kg): Mean aboveground biomass in per individual of a species;

BGB $_{\text{single,average}}$ (kg): Mean belowground biomass in per individual of a species;

Individuals: Estimated number of individuals of a single species.

The ratio between total aboveground and total belowground biomass of different tree species was calculated to better interpret the results and preferences derived from different models. The formula for calculating was as follows:

$$\text{AGB (or BGB)ratio (\%)} = \frac{\text{AGB (or BGB)}}{\text{Total Biomass}}$$

where,

AGB: Total aboveground biomass for single species;

BGB: Total belowground biomass for single species.

Finally, the AGB and BGB of different species were converted into organic carbon content based on the reference, with corresponding conversion coefficients provided in Table S2. The cumulative carbon stock (t C) was then calculated by summing the AGB and BGB carbon stock for each species.

$$\text{Cumulative Estimated Carbon stock (t C)} = \sum \frac{\text{Species Biomass}_{\text{AGB, T}}\,(\text{kg}) \times \text{CF}}{1000} + \sum \frac{\text{Species Biomass}_{\text{BGB, T}}\,(\text{kg}) \times \text{CF}}{1000}$$

The formula used to calculate the carbon stock after two years of mangrove reforestation within the sampling plot is as follows:

$$\textit{EstimatedCarbonStock}(tC) = \textit{CrbonStock}_{2024} - \textit{CrbonStock}_{2022}$$

The annual carbon sequestration rate (t C $yr^{-1}$) was estimated as the difference in carbon stock between two consecutive years, calculated using the following formula:

$$\textit{AnnualCarbonSequestrationRates}(tCyr^{-1}) = \textit{CarbonStock}_{(t+1)} - \textit{CarbonStock}_{(t)}$$

where $t$ represents the year of measurement. This approach assumes a linear accumulation of carbon within the one-year interval.

The amount of CO2 sequestration was calculated by the formula as follows:

$$\text{Estimated } CO_2 \text{ Sequestration (t } CO_2 \text{ eq )} = \text{Estimated Carbon Stock} \times \frac{44}{12}$$

where, the molecular weight of $CO_2$ is 44, and the molecular weight of carbon (C) is 12.

### 2.4. Normalized Difference Vegetation Index (NDVI)

Assessing carbon stock using satellite-derived area estimation is a convenient, non-destructive, and minimally invasive method recently adopted by multiple carbon trading certification and assessment systems (Myeong et al., 2006). This study utilizes remote sensing techniques to calculate the Normalized Difference Vegetation Index (NDVI) using Sentinel-2 satellite imagery. NDVI values were analyzed on four key dates — September 15, 2022; December 24, 2022; December 29, 2023; and January 2, 2025 — selected based on two criteria: cloud coverage below 10 % to minimize atmospheric interference and low tide conditions to enhance the visibility of coastal and intertidal vegetation. Sentinel-2 Level-1C (L1C) imagery was obtained from the Copernicus Data Space Ecosystem (https://browser.dataspace.copernicus.eu/), providing top-of-atmosphere reflectance values suitable for NDVI computation. NDVI was calculated using the formula (NIR − RED) / (NIR + RED), where Band 8 (Near-Infrared, NIR) and Band 4 (Red, RED) were used for the computation. The NDVI function in ArcGIS Pro 3.4.2 was employed to perform the calculations. The average NDVI was calculated from our five sampling sites to assess the trends in mangrove growth.

Subsequently, the vegetation coverage area of the monitoring sites was assessed using NDVI value. Due to this approach's lack of species-level identification capability, the carbon stock estimates were conducted using the global average mangrove carbon stock standard of 15.2 t C $ha^{-1}$ $yr^{-1}$. The calculation formula is presented as follows:

$$\text{Estimated Carbon Stock}\left(\text{t C yr}^{-1}\right) = 15.2\left(\text{t C ha}^{-1}\text{yr}^{-1}\right) \times \text{Recognizable image coverage area (ha)}$$

### 2.5. Statistical analysis

Independent-sample t-tests were conducted to evaluate differences in reforestation types (Area A, B, and the total area), time periods, and various assessment variables, including: (1) interannual differences in biomass models estimation and carbon sequestration rates; (2) differences in carbon sequestration rates between reforestation types; (3) variation in cumulative biomass estimates produced by different models; and (4) differences between NDVI values and cumulative biomass at each time point. All statistical analyzes were performed using Python (v3.11) with the SciPy and Seaborn libraries. A significance threshold of $p$-value $< 0.05$ was used to determine statistical significance.

## 3. Results

### 3.1. The population dynamics and biomass estimation

The planting area, annual density, surviving individuals, average height, and basal diameter variations for each mangrove species within the study area are presented in Table 1. The results indicated that the

**Table 1**
The planting area, annual density, surviving individuals, average height, and basal diameter variations for each mangrove species within the study area.

| Timeline / Species | Actual Planting Area (ha) | Individual (Ind.)) | | | Surviving Density (ind. / ha | | | Estimated Surviving Planted Individuals (ind.) | | | Average tree height (H) (m) | | | Average basal diameter (D) (cm) | | |
|---|---|---|---|---|---|---|---|---|---|---|---|---|---|---|---|---|
| | | D-22 | D-23 | D-24 | D-22 | D-23 | D-24 | D-22 | D-23 | D-24 | D-22 | D-23 | D-24 | D-22 | D-23 | D [a] −24 |
| *Aegiceras corniculatum* | 9.10 | 8 | 6 | 6 | 2,222 | 1,667 | 1,667 | 20,218 | 15,163 | 15,163 | **0.40 ± 0.09** [b] | **0.85 ± 0.03** [b] | **0.92 ± 0.05** [b] | 1.04 ± 0.26 | 1.47 ± 0.33 | 1.91 ± 0.18 |
| *Avicennia marina* | 4.28 | 24 | 17 | 16 | 13,333 | 9,444 | 8,889 | 57,067 | 40,422 | 38,044 | 0.69 ± 0.09 | 0.84 ± 0.09 | 0.93 ± 0.08 | 0.83 ± 0.15 | 1.83 ± 0.47 | 2.57 ± 0.52 |
| *Bruguiera gymnorrhiza* | 5.32 | 3 | 2 | 2 | 1,111 | 741 | 741 | 5,907 | 3,938 | 3,938 | 0.41 ± 0.08 | 0.80 ± 0.04 | 0.86 ± 0.09 | 1.45 ± 0.04 | 2.27 ± 0.02 | 2.39 ± 0.16 |
| *Kandelia obovata* | 9.10 | 35 | 34 | 33 | 9,722 | 9,444 | 9,167 | 88,452 | 85,924 | 83,397 | 0.49 ± 0.14 | 0.62 ± 0.10 | 0.95 ± 0.13 | **1.11 ± 0.26** [b] | **2.58 ± 0.44** [b] | **3.96 ± 0.55** [b] |
| *Rhizophora stylosa* | 3.78 | 2 | 1 | – | 1,111 | 556 | – | 4,200 | 2,100 | – | 0.46 ± 0.03 | 0.69 ± 0.00 | – | 1.50 ± 0.40 | 3.30 ± 0.00 | – |

[a] D represents December, and the following number represents the year.
[b] Bold numbers represent species with the highest rate of change.

primary source of spatial variability was attributable to specise composition at each site, specifically the differences between mixed and monoculture forests areas, rather than to physical environmental factors. An initial planting count of 175,842 individuals in 2022, with the range of average height from 0.40 to 0.69 m and basal diameter from 0.83 to 1.50 cm. Until 2024, approximately 140,000 individuals survived, corresponding to an overall survival rate of around 79.92 %. Average height increased significantly to between 0.86 and 0.95 m, with the range of basal diameter from 1.91 to 3.96 cm. Survival rates by species (Fig. 2) revealed that *K. obovata* exhibited the highest survival rate (97.14 % in 2023; 94.29 % in 2024). In contrast, *R. stylosa* experienced the highest mortality, with no surviving individuals recorded in sampling areas by 2024. Regarding growth rates, *A. corniculatum* demonstrated the greatest height increase (0.52 m over two years), while *Kandelia obovata* showed the greatest increase in basal diameter (2.85 cm over two years).

Species-specific average individual and total biomass estimated derived from two allometric models were summarized in Table S3, S4 and S5. Using Model I, *B. gymnorrhiza* exhibited the highest AGB increment, averaging 1.57 kg per individual over two years, while *K. obovata* showed the highest BGB increment, averaging 0.71 kg per individual. Overall, *B. gymnorrhiza* demonstrated the greatest total biomass increment, averaging 1.62 kg per individual over two years. In contrast, Model II indicated that *A. marina* displayed the highest increases in both AGB and BGB, averaging 1.68 kg and 3.06 kg per individual over two years, respectively, resulting in a total biomass increment of 4.74 kg per individual.

The annual variation in AGB and BGB biomass for each species estimated by the two models were present in Fig. 3. Fig. 3A represents the biomass partitioning based on Model I, highlighting a predominant investment in aboveground biomass during the early plantation stage, except for *K. obovata*, that BGB biomass proportion increased from 63 % to 68 % between 2023 and 2024. Among species assessed, *B. gymnorrhiza* demonstrated the highest proportion of AGB, ranging from 92 % to 96 % of total biomass. Conversely, Fig. 3B reveals an opposite trend which was calculated by Model II, with most species emphasizing BGB biomass accumulation (≥50 % of total biomass), except for *A. corniculatum,* which maintained a greater proportion of AGB.

### *3.2. Cumulative carbon stock estimates and sequestration rates based on Model I and II*

Table 2 summarizes the results of cumulative carbon stock, which was calculated based on Model I and Model II, while the corresponding cumulative estimated $CO_2$ sequestration amounts are provided in Table 3. Although these estimates are based on biomass conversion, temporal changes were used to calculate annual sequestration rates, which provide a more dynamic and meaningful indicator of early-stage carbon gain. According to Model I, the cumulative increase in carbon stock over two years was 45.34t C (averaging 3.39 t C $ha^{-1}$). Specifically, carbon sequestration increased from 13.32t C $yr^{-1}$ in 2022 – 2023 to 32.03 t C $yr^{-1}$ in 2023–2024, representing a 2.40 times difference between the two periods. In contrast, Model II estimated a total cumulative carbon stock of 94.77 t C (averaging 7.08 t C $ha^{-1}$) with annual sequestration increasing from 37.34 t C $yr^{-1}$ to 57.42 t C $yr^{-1}$. An approximate 1.54 times difference between two periods.

Further comparative analysis of the carbon stock contributions depended on the two models (Fig. 4) revealed notable differences in evaluating species-specific carbon stock capacities. Particularly, *K. obovata* and *A. marina* exhibited superior carbon stock capabilities in Model I and Model II, respectively. Conversely, *A. corniculatum* and *B. gymnorrhiza* demonstrated the lowest carbon stock capacities within the two models.

Subsequently, carbon sequestration performance was compared across different reforestation types, years, and assessment models

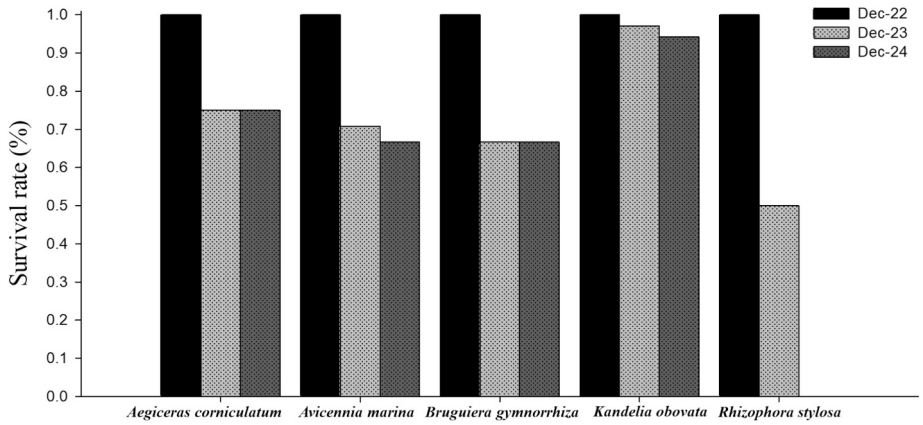


**Fig. 2.** Survival rates by species in different years.

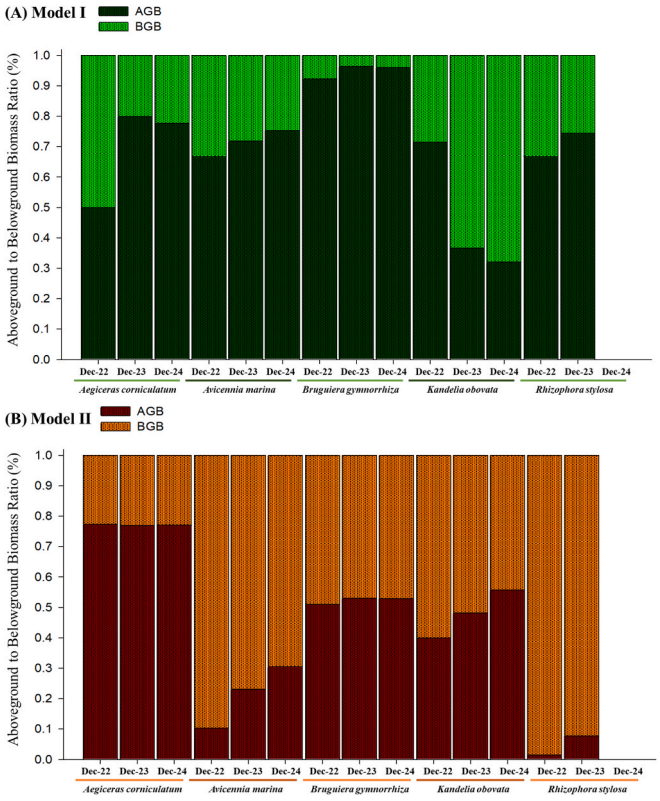


**Fig. 3.** The annual variation in AGB (Aboveground biomass) and BGB (Belowground biomass) biomass for each species estimated by the two models. Model I, derived from equations established for mangrove saplings across various sites in China. Model II, utilizing species-specific biomass equations. (A) The biomass partitioning based on Model I; (B) The biomass partitioning based on Model II.

(Fig. 5). Species-specific annual carbon sequestration rates are detailed in Table S5. The results revealed a consistent upward trend across all areas and under both models, with carbon sequestration rates in the second year exceeding those in the first. Although this trend was not statistically significant (Model I: $t = -2.79$, $p = 0.108$; Model II: $t = -3.62$, $p = 0.069$), the observed increases suggest early-stage carbon accumulation dynamics during mangrove establishment.

When comparing the two models within the same year, Model II consistently produced higher estimates than Model I. A closer examination revealed that Model I estimated substantially higher carbon sequestration rates in Area A compared to Area B, especially in the second year. In contrast, Model II suggested the opposite pattern, with higher rates observed in monoculture plantations. This divergence highlights the potential for model selection to introduce estimation bias and obscure the actual effectiveness of different planting strategies.

Although the differences were not statistically significant, the overall findings suggest that juvenile mangrove stands exhibit a phase of rapid carbon accumulation during the early stages of growth, which may offer important advantages for carbon offset initiatives.

**Table 2**
Comparison of cumulative carbon stock estimates based on Model I and Model II.

| Species | Model I Cumulative Estimated Carbon Stock (t C) | | | Model II Cumulative Estimated Carbon Stock (t C) | | |
|---|---|---|---|---|---|---|
| | Dec-22 | Dec-23 | Dec-24 | Dec-22 | Dec-23 | Dec-24 |
| *Aegiceras corniculatum* | 0.16 | 0.33 | 0.56 | 1.83 | 3.09 | 5.43 |
| *Avicennia marina* | 0.70 | 4.43 | 11.95 | 26.26 | 54.65 | 89.83 |
| *Bruguiera gymnorrhiza* | 0.35 | 2.32 | 3.19 | 1.29 | 2.29 | 2.58 |
| *Kandelia obovata* | 2.53 | 9.80 | 33.44 | 1.69 | 10.29 | 34.90 |
| *Rhizophora stylosa* | 0.05 | 0.23 | – | 6.90 | 4.99 | – |
| Total | **3.79** | **17.11** | **49.14** | **37.97** | **75.31** | **132.74** |

**Table 3**
Comparison of cumulative $CO_2$ sequestration estimates based on Model I and Model II.

| Species | Model I Cumulative Estimated $CO_2$ Sequestration (t $CO_2$ eq) | | | Model II Cumulative Estimated $CO_2$ Sequestration (t $CO_2$ eq) | | |
|---|---|---|---|---|---|---|
| | Dec-22 | Dec-23 | Dec-24 | Dec-22 | Dec-23 | Dec-24 |
| *Aegiceras corniculatum* | 0.60 | 1.22 | 2.06 | 6.71 | 11.34 | 19.91 |
| *Avicennia marina* | 2.55 | 16.24 | 43.80 | 96.30 | 200.37 | 329.37 |
| *Bruguiera gymnorrhiza* | 1.29 | 8.50 | 11.69 | 4.72 | 8.39 | 9.47 |
| *Kandelia obovata* | 9.26 | 35.93 | 122.60 | 6.19 | 37.74 | 127.95 |
| *Rhizophora stylosa* | 0.20 | 0.84 | – | 25.29 | 18.30 | – |
| Total | **13.90** | **62.72** | **180.15** | **139.22** | **276.14** | **486.70** |

### 3.3. Changes in reforested area and evaluation of carbon stock using remote sensing techniques

Fig. 6 illustrates the spatial changes in vegetation cover based on the NDVI in the study area, with the red triangle pointing to the sampling location. Fig. 6A shows the initial condition of the study site and

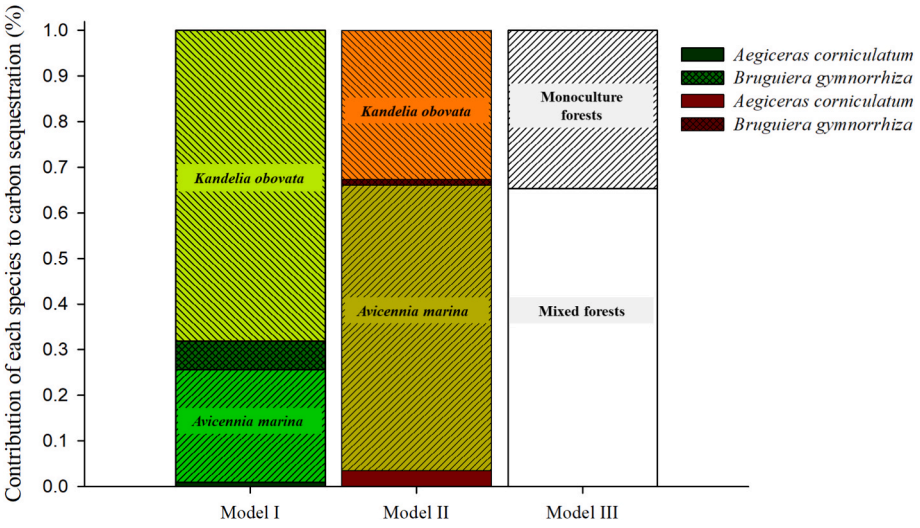


**Fig. 4.** Cumulative carbon stock contributions estimated using Model I, II and III. Model I and II represent species-specific contributions to carbon sequestration (indicated by different colors), whereas Model III illustrated contributions under different planting strategies (monoculture vs. mixed forests).

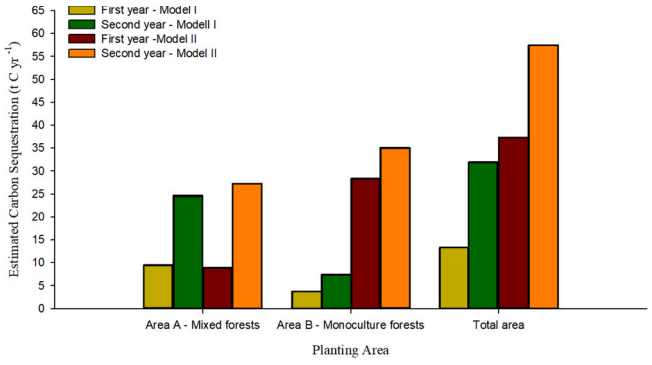


**Fig. 5.** Comparison of annual carbon sequestration rates (t C $yr^{-1}$) across different reforestation types (Area A – mixed forests; Area B – monoculture forests; Total area), assessment models (Model I and Model II), and period of monitoring years (Year 1 and Year 2).

adjacent areas, dominated by dark green pixels representing *S. alterniflora* coverage, with the highest NDVI value (0.18) and the area totaling 13.07 ha. Following removal of *S. alterniflora* and subsequent reforestation with mangrove saplings (Fig. 6B), no significant NDVI value (−0.04) was initially detectable in satellite imagery. Approximately a year after planting (Fig. 6D), light green patches or lines began to emerge, indicating early vegetation growth (NDVI = 0.06). After two years (Fig. 6F), the satellite imagery showed substantial greening within the reforested area, represented by a distinct increase in dark green pixels (NDVI = 0.138). Satellite imagery and NDVI variation in whole area (Fig. 7 Green line) clearly demonstrated vegetation development over the analyzed timeline. Ultimately, the total reforested area was assessed as 10.45 ha, including 6.83 ha of mixed forests and 3.62 ha of monoculture forests (Table 4).

Subsequently, this assessed area was utilized to estimate carbon stock capacity. Under the initial conditions dominated by *S. alterniflora*, the carbon sequestration potential was estimated at 317.99 t C, equivalent to 1,165.97 t $CO_2$eq. Following mangrove reforestation, the cumulative estimated carbon stock backed to 158.84 t C, corresponding to a $CO_2$ sequestration rate of 582.41 t $CO_2$eq (Table 4).

### *3.4. Comparison of allometric models and NDVI for evaluating carbon dynamics in restored mangroves*

Table 4 was indicated to carbon stock and carbon sequestration estimates derived from three different models across reforested areas during two years. A consistent trend was observed, with Model III producing the highest estimates, followed by Model II and then Model I. Interestingly, although the area detected by satellite remote sensing (Model III) was smaller than the actual measured planting area, its estimated of both carbon stock and carbon sequestration were the highest. Fig. 4 further indicated that only Model I and Model II were capable of providing detailed information on species-specific contributions, whereas Model III, when combined with field observations, was able to highlight differences among planting strategies but could not resolve the role of individual species. Therefore, while Model III offers advantages in terms of convenience and scalability, its application remains limited compared with the more species-explicit assessments provided by Model I and Model II.

Considering all results, Model I was deemed more suitable for evaluating biomass accumulation during the juvenile stage of the restored mangrove community in this study. To further clarify the limitations of the NDVI methodology, the temporal trends of cumulative biomass (AGB + BGB) estimated using Model I were compared with NDVI variations across different reforestation types (Fig. 7). Both NDVI and biomass increased over time, with Area A consistently exhibiting greater biomass accumulation than Area B.

To further assess differences among reforestation types, independent-sample t-tests were performed on NDVI and biomass values at each time point (Fig. 8). The results showed that biomass accumulation was consistently and significantly greater in Area A than in Area B across all valid time points ($p < 0.0001$). In contrast, NDVI values did not differ significantly between reforestation types after 2022, despite clear trends in biomass. This indicates that while mixed-species plantations promote more rapid and substantial early-stage biomass accumulation, NDVI may not reliably capture such differences, particularly in structurally complex and species-diverse forest systems.

## 4. Discussion

### *4.1. Refining carbon stock estimates for early growth stages to improve the assessment of mangrove carbon dynamics*

Considering that tree growth involves both aboveground and

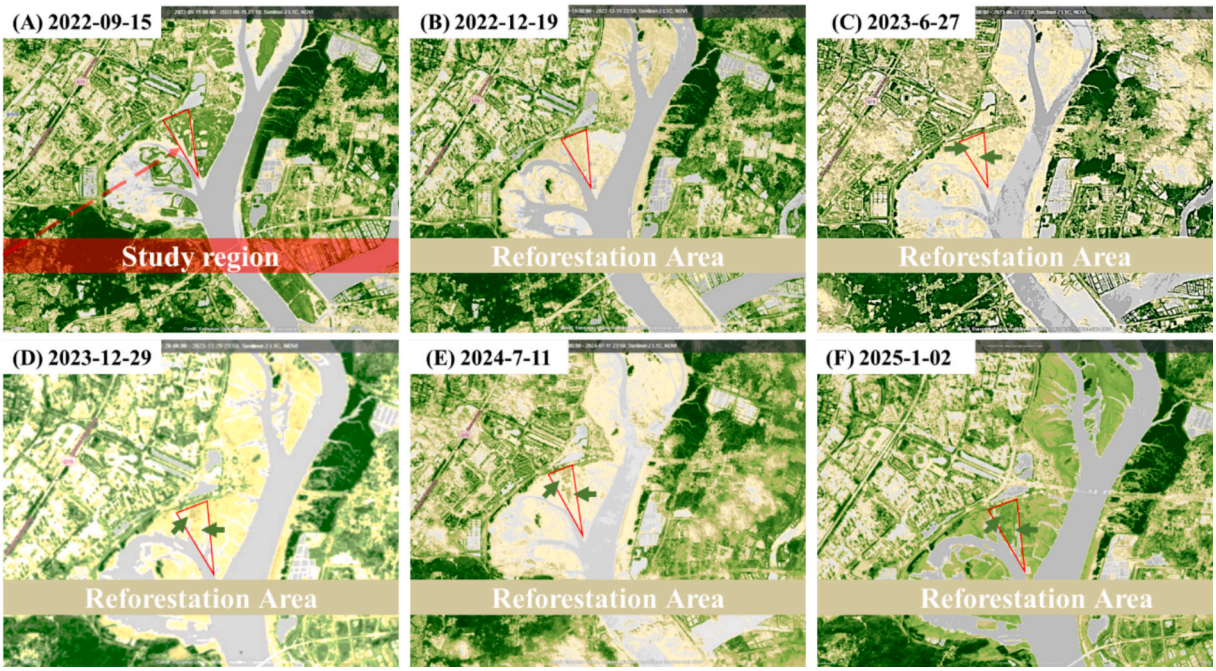


**Fig. 6.** The spatial changes in vegetation cover based on the NDVI in the study area, with the red triangle pointed to the sampling location. (A) The initial condition of vegetation cover in the study site and adjacent areas; (B) The condition of the removal of *S. alterniflora* and subsequent reforestation with mangrove saplings; (C-D) The condition of vegetation cover approximately 0.5 and 1 year after reforestation; (E-F) The condition of vegetation cover approximately 1.5 and 2 year after reforestation.

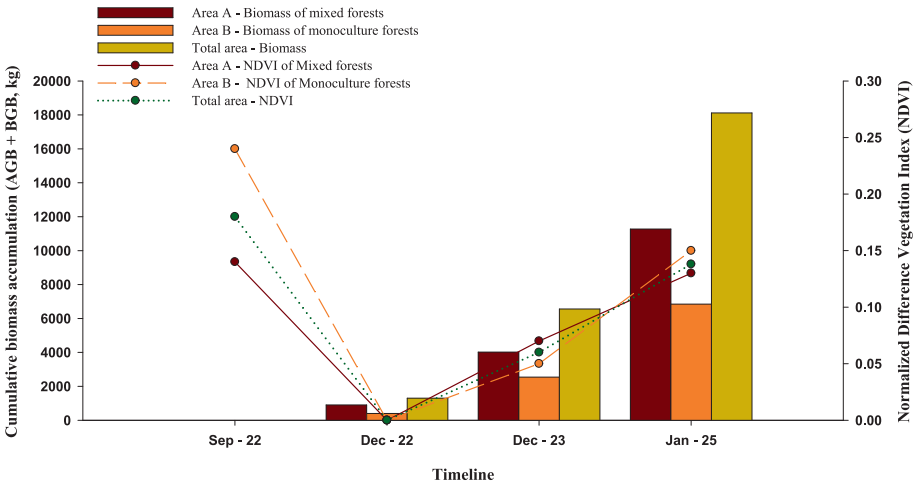


**Fig. 7.** Temporal trends of cumulative biomass accumulation (AGB + BGB) and Normalized difference vegetation index (NDVI) across reforested areas. Bar plots represent cumulative biomass (kg) estimated using Model I for Area A (mixed forests), Area B (monoculture forests), and the total area. Line plots denote the corresponding NDVI values for each reforestation type.

**Table 4**
Comparison of cumulative carbon stock and $CO_2$ sequestration estimates under different planting strategies based on Model I, Model II, and Model III.

| Area type | Actual Planting Area | Remosence Area | Cumulative Estimated Carbon Stock (t C) | | | Cumulative Estimated $CO_2$ Sequestration (t $CO_2$ eq) | | |
|---|---|---|---|---|---|---|---|---|
| | | | Model I | Model II | Model III | Model I | Model II | Model III |
| Mixed forests (A) | 9.10 | 6.83 | 34.10 | 31.20 | 103.82 | 125.03 | 114.42 | 380.66 |
| Monoculture forests (B) | 4.28 | 3.62 | 11.25 | 63.57 | 55.02 | 41.25 | 233.07 | 201.75 |
| Total | 13.38 | 10.45 | **45.35** | **94.77** | **158.84** | **166.28** | **347.49** | **582.41** |

belowground root systems, biomass assessments commonly distinguish and separately quantify these two biomass components. Additionally, recent findings indicate that, on average, biomass accumulation is influenced nearly equally by different tree-age components, forest maturation, and productivity increases (Carnell et al., 2022; Walcker et al., 2018). Therefore, stand age, biomass accumulation patterns and species composition require particular emphasis in carbon stock studies.

The results of this study also highlighted discrepancies between

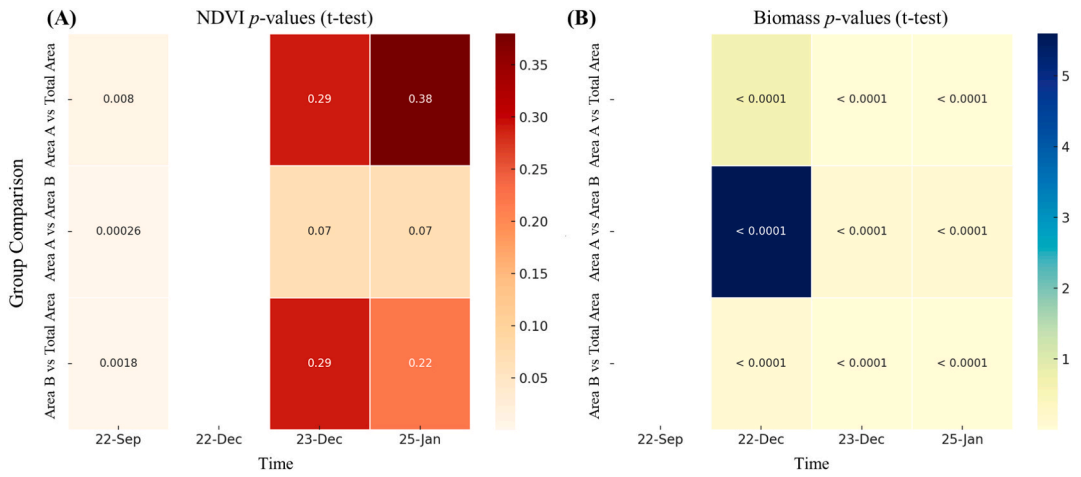


**Fig. 8.** Heatmaps of p-values from independent-sample t-tests comparing NDVI (A) and cumulative biomass (B) between reforestation types (Area A – Mixed forests, Area B – Monoculture forests, and the total area) across different time points. NDVI differences were statistically significant only in the early stage (Sep – 22), which corresponded to the *Spartina alterniflora* invasion period; therefore, biomass was not included in the analysis or discussion for that time point.

biomass estimation models, where Model II consistently yielded higher biomass estimates compared to Model I. The detail of these two distinct equations reveals that Model I accounts explicitly for the simultaneous development of root expansion, stem growth, and leaf development typical of juvenile mangroves, resulting in greater allocation to above-ground biomass accumulation. Consequently, this model emphasizes the combined growth parameters of plant height and basal diameter. In contrast, Model II was specifically developed based on larger, mature trees (DBH $\geq$ 4 cm), and its equation structure predominantly considers the growth of diameter at breast height (DBH) or basal diameter while ignoring tree height data (Hossain et al., 2016; Perera et al., 2011). This omission introduces biases between the two estimation methods, subsequently influencing carbon stock assessments. Notably, both models showed an overall upward trend in annual carbon sequestration rates; however, the differences between years were not statistically significant, likely due to the limited number of evaluation units. Nonetheless, Model II consistently yielded higher estimates, particularly in monoculture area, indicating that model selection was also an important factor influencing the interpretation of outcomes.

Further analysis of species-specific carbon sequestration patterns revealed that *K. obovata* with relatively smaller discrepancies between the two models compared to other species. This trend appeared to be closely associated with the biological and ecological traits of *K. obovata*. As a pioneer mangrove species, it is characterized by rapid growth and high productivity. In particular, during the early establishment stage, its short leaf longevity reflects a greater allocation of biomass to stem and root development (Khan and Kabir, 2017). The result of this study also pointed *K. obovata* demonstrated accelerated diameter growth in the first year, followed by more balanced increments of both height and diameter in the second year. Because both models apply weighted functions to diameter and height parameters, their estimates for this species remained relatively consistent. Moreover, *K. obovata* contributed the largest cumulative proportion of carbon sequestration among all species in model I, likely due to its higher initial planting density and superior survival rate within the restoration site. Collectively, these findings indicate that the differences in carbon sequestration estimates for *K. obovata* derived from the two models were not anomalies, but rather reflect the intrinsic growth dynamics and stand structure of this species during the early restoration phase. These results further highlight that planting strategy and species composition are the primary sources of spatial variability under uniform environmental conditions.

On the other hand, illustrating potential mangrove coverage using NDVI coefficients to estimate carbon stock, has recently been a common evaluation approach (Suardana et al., 2023). In this study, we introduced NDVI-based estimations as Model III. Despite its relatively low average NDVI values and vegetation coverage, Model III yielded the highest carbon stock among the models evaluated. The bias result likely due to the carbon stock conversion factor applied accounts for both biomass and soil carbon stocks simultaneously (Myneni et al., 1995).

Moreover, several studies have highlighted the inherent limitations of NDVI, particularly its tendency to deviate in reflectance under varying vegetation densities, which can lead to biased estimates of carbon stocks (Baloloy et al., 2018; Bindu et al., 2020; Hartoyo et al., 2022; Razali et al., 2019; Suardana et al., 2023). To investigate this issue, this study further conducted a comparative analysis between NDVI values and cumulative biomass estimates. The results indicated that NDVI did not reliably reflect actual biomass accumulation and spetial heterogeneity, particularly during the initial planting stage, where notable discrepancies were observed. Several factors may explain this inconsistency: (1) Limitations in NDVI Reflectance Sensitivity: Previous studies have highlighted that NDVI has inherent limitations in detecting both sparse and high-density vegetation. Specifically, when the tree canopy area is small or the Leaf Area Index (LAI) is below 2 $m^2/m^2$, the sensitivity of NDVI to vegetation changes significantly decreases, potentially leading to underestimation of actual area in vegetation (Goswami et al., 2015). Conversely, in high biomass conditions, NDVI tends to saturate, rendering it less responsive to further increases in vegetation area (Gao et al., 2023). In our study, the average leaf width of different tree species ranged from 8.00 $\pm$ 2.62 cm to 17.33 $\pm$ 2.49 cm (mean: 10.14 $\pm$ 4.34 cm). Despite noticeable growth in canopy width over the two-year period (Table S7), the chlorophyll reflectance activity remained relatively low, resulting in lower NDVI values. (2) Variability of NDVI Values: Ruan et al. (2022) reported considerable regional variability in mangrove NDVI, with the highest average NDVI value of 0.80 recorded in Asian mangroves and the lowest (0.67) in African mangroves. Additionally, global data from 2000 to 2018 indicate a slow yet gradual increase in annual average NDVI values for mangroves. Furthermore, variations in NDVI have been used to reflect vegetation health status, where healthier vegetation generally exhibits higher NDVI values, and unhealthy vegetation shows reduced NDVI. These findings all pointed to the feature with dynamic nature of NDVI. (3) Limited Monitoring Capability of NDVI for Complex Forest Structures: NDVI primarily reflects chlorophyll content and is less sensitive to vertical structural changes such as species compostion, tree height and basal diameter. This limitation hinders its ability to accurately represent biomass accumulation in forests, particularly in young or structurally immature forests (Goswami et al., 2015). (4) Lack of suitable NDVI – Carbon Stock Calibrated Relationships: Current studies have

predominantly utilized regression analyses correlating NDVI with metrics such as aboveground biomass (AGB) (Baloloy et al., 2018), aboveground carbon (AGC) (Suardana et al., 2023), or vegetation density (Hartoyo et al., 2022; Razali et al., 2019) to calibrate NDVI against field-measured carbon stocks. These studies have emphasized the significant role of location and environmental conditions in influencing the accuracy and reliability of calibration results, resulting in considerable variability in performance across different mangrove ecosystems (Değermenci and Zengin, 2023). Furthermore, these previous investigations have primarily focused on mature mangrove forests, making their calibration methodologies less suitable for accurately estimating carbon stocks in younger or mixed-age mangrove stands.

In summary, although this study provides approximately two years of monitoring data, the current temporal and spatial resolution remains insufficient, particularly for further analysis of the relationship between NDVI and canopy closure. Fortunately, field monitoring in the study area is ongoing. With the support of a larger-scale dataset, future research will focus on integrating ground-based measurements with remote sensing observations using multi-source data fusion approaches to develop NDVI correction methodologies. This will help improve the accuracy and applicability of NDVI in mangrove carbon assessments. Until then, the use of NDVI as a proxy for carbon stock estimation should be approached with caution, particularly in reforested area, and should be interpreted in conjunction with field-based measurements.

### 4.2. The reforestation planting strategy

Seedling recruitment is critical for mangrove regeneration and long-term ecosystem function (George et al., 2019; Srivastava and Bal, 1984). In this study, a high planting density (~27,500 individuals $ha^{-1}$) was applied to suppress *Spartina alterniflora* reinvasion, and sapling density remained above 20,000 individuals $ha^{-1}$ after two years, indicating strong survival and regeneration potential. This strategy aligns with national restoration guidelines, which recommend densities between 6600 and 10,000 individuals $ha^{-1}$ depending on developmental stage (Liu and Ma, 2024).

Otherwise, monoculture plantations are still commonly used for their simplicity and visual uniformity, mixed-forests approaches offer notable ecological advantages. In this study, mixed mangrove stands exhibited high survival rates, stable structural development and higher annual carbon sequestration rate. These findings support previous research advocating for species-diverse plantations to enhance ecosystem resilience, biodiversity, sediment carbon stock, and resistance to environmental stressors (Alongi, 2011; Rai et al., 2021).

Based on these results, three key considerations are recommended for subtropical mangrove restoration projects: (1) Selection of planting materials: Due to the high mortality rates of propagules or seedlings, saplings should be used to maintain stable densities and offset slower subtropical growth, thereby accelerating carbon stock development. (2) Planting density: High densities help suppress invasive species, but continued monitorind and management are needed to refine optimal density target. (3) Mixed plantation: Mixed-species strategies enhance forest stability, survival, and carbon sequestration. Species selection should be guided by historical distribution records and site-specific ecological suitability.

### 4.3. Reforested in Quanzhou Bay: A blue carbon model for corporate Social Responsibility (CSR) and long-term feasibility

Mangrove ecosystems are widely recongnized as efficient coastal carbon sinks and play a central role in blue carbon strategies (Zhu & Yan, 2022). International certification frameworks such as Verra's Verified Carbon Standard (VCS) and the Gold Standard specifically emphasize carbon accounting during early to mid-successional stages (10–30 years), thereby making early corporate investment in juvenile mangrove reforestation a strategic opportunity. Through these opportunities, corporations can engage in mangrobe restoration as a part of their CSR commitments, while simultaneously contributing to carbon neutrality in alignment with the United Nations Sustainable Development Goals (SDGs).

In this case was a project supported by the Mangrove Conservation Foundation (MCF), Shenzhen, whose primary funding is derived from corporate sponsorship, serving as a strong demonstration of CSR in action. Although the early-stage reforested stands in this study currently appeared carbon stock lower compared to global averages for the mature mangroves, this was attributed to the juvenile colonization stage. With continued forest development, carbon stock will expected to increase steadily, highlighting the potential long-term carbon benefits that can ultimately provide returns to corporate investors.

However, the practical implementation of carbon credit certification and its potential return to corporate investors remain constrained by several challenges. (1) Practical challenge to carbon credit certification: Certification typically requires long-term datasets. But local cultural contexts, site conditions, and monitoring standards may not fully match with the stringent requirements of international framworks. These limitations highlight the importance of supportive local policy mechanisms, including the development of region-specific blue carbon accounting standards, government-backed incentives, and stronger public–private partnerships to enhance certification feasibility. (2) Robust monitoring, reporting, and verification (MRV): Long-term monitoring is essential to ensure the credibility of carbon sequestration estimates. Although some certification organizations recognize NDVI-based approaches for estimating carbon stocks recently, the results of this study indicared that NDVI alone is unreliable at the juvenile stage. Instead, integrating remote sensing with field surveys is essential for producing accurate and verifiable long-term data. Without such mechanisms, the contribution of reforested mangroves to carbon markets and CSR commitments may risk being overestimated.

## 5. Conclusions

This study integrated three carbon stock assessment methods to evaluate the carbon storage potential of reforested mangroves during the early developmental stage. Given that many current mangrove restoration projects begin with young saplings, the dynamic growth characteristics of juvenile forests must be explicitly considered, especially when their carbon stock capacity is intended for participation in carbon markets. To address this, we propose a phased framework for carbon stock assessment in restoration areas: (1) Short-Term Assessment: Applicable to mangrove stands with a diameter at breast height (DBH) $< 4$ cm. In this stage, biomass estimation using Model I or species-specific juvenile allometric equations is recommended. While this approach is limited to the initial years of growth, it more accurately captures early-stage biomass dynamics, avoids overestimation, and better reflects actual carbon accumulation potential. (2) Long-Term Assessment: For mangrove stands with DBH $\geq 4$ cm, Model II is more appropriate, as it reflects greater energy allocation to belowground biomass and represents a more stable and robust estimate of long-term carbon storage. (3) Remote Sensing-Based Monitoring: Due to current calibration limitations, Model III (NDVI-based estimation) is more suited for monitoring mature stands and assessing large-scale carbon stocks. Its application to juvenile forests should await the development of robust NDVI calibration models that can capture early growth-stage variability.

In addition to methodological recommendations, this study identifies several critical research directions: (1) the development of comprehensive allometric growth equations across species and developmental stages to improve lifecycle-based carbon estimation, and (2) the calibration of stand-specific biomass–carbon relationships, especially for young mangrove stands where current models remain insufficient.

Finally, the Quanzhou Bay restoration project illustrates the potential of mangrove reforestation as a scalable model for integrating ecological restoration with corporate sustainability strategies and

market-based carbon finance. This case hightlight opportunities to advance CSR commitments and SDGs targets, while also emphasizing the need for long-term monitoring, robust certification mechanisms, and supportive policy framworks to ensure feasibility and credibility.

## CRediT authorship contribution statement

**Yi-Jia Shih:** Writing – review & editing, Methodology, Investigation, Conceptualization. **Kai Liu:** Writing – original draft, Investigation, Formal analysis, Data curation. **Shu-Chiang Huang:** Methodology, Conceptualization. **Yi Chang:** Validation, Methodology. **Fen-Fen Ji:** Investigation, Formal analysis. **Chun-Xi Cao:** Supervision, Methodology. **Mou-Xin Ye:** Supervision, Methodology. **Yi-Min Li:** Methodology. **Yi-Hua Jin:** Visualization. **You-Rong Yao:** Methodology.

## Funding

This study was supported by the public welfare projects (grant numbers: S23393, S24359) from the Mangrove Conservation Foundation, Shenzhen, China.

## Declaration of competing interest

The authors declare that they have no known competing financial interests or personal relationships that could have appeared to influence the work reported in this paper.

## Acknowledgements

The authors extend their sincere appreciation to Tmall Home Carnival, Alibaba Philanthropy, and the “Goods for Good” sellers for their generous contributions to the reforestation initiative. Special thanks are also given to Mr. Jin-jiang Chen and his team for his dedicated efforts in the reforestation work.

## Appendix A. Supplementary data

Supplementary data to this article can be found online at https://doi.org/10.1016/j.ecolind.2025.114126.

## Data availability

Data will be made available on request.

## References

Alongi, D.M., 2011. Carbon payments for mangrove conservation: ecosystem constraints and uncertainties of sequestration potential. Environ. Sci. Policy 14, 462–470.
Alongi, D.M., 2012. Carbon sequestration in mangrove forests. Carbon Manage. 3, 313–322.
Alongi, D.M., 2014. Carbon cycling and storage in mangrove forests. Ann. Rev. Mar. Sci. 6, 195–219.
An, S., Gu, B., Zhou, C., Wang, Z., Deng, Z., Zhi, Y., Li, H., Chen, L., Yu, D., Liu, Y., 2007. Spartina invasion in China: Implications for invasive species management and future research. Weed Res. 47, 183–191.
Baloloy, A.B., Blanco, A.C., Candido, C.G., Argamosa, R.J.L., Dumalag, J.B.L.C., Dimapilis, L.L.C., Paringit, E.C., 2018. Estimation of mangrove forest aboveground biomass using multispectral bands, vegetation indices and biophysical variables derived from optical satellite imageries: Rapideye, planetscope and sentinel-2. ISPRS Ann. Photogramm. Remote Sens. Spatial Inf. Sci. 4, 29–36.
Battocletti, V., Enriques, L., Romano, A., 2024. The voluntary carbon market: market failures and policy implications. U. Colo. l. Rev. 95, 519.
Bindu, G., Rajan, P., Jishnu, E., Joseph, K.A., 2020. Carbon stock assessment of mangroves using remote sensing and geographic information system. Egypt. J. Remote Sens. Space Sci. 23, 1–9.
Bosire, J.O., Dahdouh-Guebas, F., Walton, M., Crona, B.I., Lewis Iii, R., Field, C., Kairo, J. G., Koedam, N., 2008. Functionality of restored mangroves: A review. Aquat. Bot. 89, 251–259.
Carnell, P.E., Palacios, M.M., Waryszak, P., Trevathan-Tackett, S.M., Masqué, P., Macreadie, P.I., 2022. Blue carbon drawdown by restored mangrove forests improves with age. J. Environ. Manage. 306, 114301.
Chen, L., Wang, W., Li, Q.Q., Zhang, Y., Yang, S., Osland, M.J., Huang, J., Peng, C., 2017. Mangrove species' responses to winter air temperature extremes in China. Ecosphere 8, e01865.
Choudhary, B., Dhar, V., Pawase, A.S., 2024. Blue carbon and the role of mangroves in carbon sequestration: Its mechanisms, estimation, human impacts and conservation strategies for economic incentives. J. Sea Res. 199, 102504.
Christiansen, K.L., 2024. Relegitimising the voluntary carbon market: Visions of digital monitoring, reporting and verification. Environment and Planning A: Economy and Space, 0308518X241278937.
Değermenci, A.S., Zengin, H., 2023. Determination of carbon storage amounts in above-ground biomass using NDVI based on land use/land cover classes in Bolu. Artvin Çoruh Üniversitesi Orman Fakültesi Dergisi 24, 64–74.
Donato, D.C., Kauffman, J.B., Murdiyarso, D., Kurnianto, S., Stidham, M., Kanninen, M., 2011. Mangroves among the most carbon-rich forests in the tropics. Nat. Geosci. 4, 293–297.
Estrada-Villegas, S., Bailón, M., Hall, J.S., Schnitzer, S.A., Turner, B.L., Caughlin, T., van Breugel, M., 2020. Edaphic factors and initial conditions influence successional trajectories of early regenerating tropical dry forests. J. Ecol. 108, 160–174.
Gao, S., Zhong, R., Yan, K., Ma, X., Chen, X., Pu, J., Gao, S., Qi, J., Yin, G., Myneni, R.B., 2023. Evaluating the saturation effect of vegetation indices in forests using 3D radiative transfer simulations and satellite observations. Remote Sens. Environ. 295, 113665.
George, G., Krishnan, P., Mini, K., Salim, S., Ragavan, P., Tenjing, S., Muruganandam, R., Dubey, S., Gopalakrishnan, A., Purvaja, R., 2019. Structure and regeneration status of mangrove patches along the estuarine and coastal stretches of Kerala, India. J. For. Res. 30, 507–518.
Goswami, S., Gamon, J., Vargas, S., Tweedie, C., 2015. Relationships of NDVI, Biomass, and Leaf Area Index (LAI) for six key plant species in Barrow. Alaska, PeerJ PrePrints.
Hamilton, S.E., Casey, D., 2016. Creation of a high spatio-temporal resolution global database of continuous mangrove forest cover for the 21st century (CGMFC-21). Glob. Ecol. Biogeogr. 25, 729–738.
Hartoyo, A., Pamoengkas, P., Mudzaky, R., Khairunnisa, S., Ramadhi, A., Munawir, A., Komarudin, K., Hidayati, S., Sunkar, A., 2022. Estimation of vegetation cover changes using normalized difference vegetation index (NDVI) in Mount Halimun Salak National Park, Indonesia, IOP Conference series: earth and environmental science. IOP Publishing, p. 012068.
Hilmi, N., Chami, R., Sutherland, M.D., Hall-Spencer, J.M., Lebleu, L., Benitez, M.B., Levin, L.A., 2021. The role of blue carbon in climate change mitigation and carbon stock conservation. Front. Clim. 3, 710546.
Hong, S., Yin, G., Piao, S., Dybzinski, R., Cong, N., Li, X., Wang, K., Peñuelas, J., Zeng, H., Chen, A., 2020. Divergent responses of soil organic carbon to afforestation. Nat. Sustainability 3, 694–700.
Hossain, M., Shaikh, M.-A.-A., Saha, C., Abdullah, S.R., Saha, S., Siddique, M.R.H., 2016. Above-ground biomass, nutrients and carbon in Aegiceras corniculatum of the Sundarbans. Open J. Forest. 6, 72.
Huang, X., Duan, Y., Tao, Y., Wang, X., Long, H., Luo, C., Lai, Y., 2022. Effects of Spartina alterniflora invasion on soil organic carbon storage in the beihai coastal wetlands of China. Front. Mar. Sci. 9, 890811.
Kauffman, J.B., Cole, T.G., 2010. Micronesian mangrove forest structure and tree responses to a severe typhoon. Wetlands 30, 1077–1084.
Kauffman, J.B., Donato, D.C., 2012. Protocols for the measurement, monitoring and reporting of structure, biomass and carbon stocks in mangrove forests. Citeseer.
Keith, H., Vardon, M., Obst, C., Young, V., Houghton, R.A., Mackey, B., 2021. Evaluating nature-based solutions for climate mitigation and conservation requires comprehensive carbon accounting. Sci. Total Environ. 769, 144341.
Khan, M.N., Kabir, M.E., 2017. Ecology of *Kandelia obovata* S., L.) Yong: A Fast-Growing Mangrove in Okinawa, Japan. In: DasGupta, R., Shaw, R. (eds) Participatory Mangrove Management in a Changing Climate. Disaster Risk Reduction. Springer, Tokyo. https://doi.org/10.1007/978-4-431-56481-2_18.
Komiyama, A., Ong, J.E., Poungparn, S., 2008. Allometry, biomass, and productivity of mangrove forests: A review. Aquat. Bot. 89, 128–137.
Li, P., Liu, D., Liu, C., Li, X., Liu, Z., Zhu, Y., Peng, B., 2024. Blue carbon development in China: Realistic foundation, internal demands, and the construction of blue carbon market trading mode. Front. Mar. Sci. 10, 1310261.
Liu, J., Zhang, Z., Xu, X., Kuang, W., Zhou, W., Zhang, S., Li, R., Yan, C., Yu, D., Wu, S., 2010. Spatial patterns and driving forces of land use change in China during the early 21st century. J. Geog. Sci. 20, 483–494.
Liu, N., Ma, Z., 2024. Ecological restoration of coastal wetlands in China: Current status and suggestions. Biol. Conserv. 291, 110513.
López-Angarita, J., Roberts, C.M., Tilley, A., Hawkins, J.P., Cooke, R.G., 2016. Mangroves and people: Lessons from a history of use and abuse in four Latin American countries. For. Ecol. Manage. 368, 151–162.
Lunstrum, A., Chen, L., 2014. Soil carbon stocks and accumulation in young mangrove forests. Soil Biol. Biochem. 75, 223–232.
Macreadie, P.I., Anton, A., Raven, J.A., Beaumont, N., Connolly, R.M., Friess, D.A., Kelleway, J.J., Kennedy, H., Kuwae, T., Lavery, P.S., 2019. The future of Blue Carbon science. Nat. Commun. 10, 3998.
Macreadie, P.I., Costa, M.D., Atwood, T.B., Friess, D.A., Kelleway, J.J., Kennedy, H., Lovelock, C.E., Serrano, O., Duarte, C.M., 2021. Blue carbon as a natural climate solution. Nat. Rev. Earth Environ. 2, 826–839.
Mardani, A., Streimikiene, D., Cavallaro, F., Loganathan, N., Khoshnoudi, M., 2019. Carbon dioxide (CO2) emissions and economic growth: A systematic review of two decades of research from 1995 to 2017. Sci. Total Environ. 649, 31–49.
Mcleod, E., Chmura, G.L., Bouillon, S., Salm, R., Björk, M., Duarte, C.M., Lovelock, C.E., Schlesinger, W.H., Silliman, B.R., 2011. A blueprint for blue carbon: Toward an

improved understanding of the role of vegetated coastal habitats in sequestering CO2. Front. Ecol. Environ. 9, 552–560.
Mora, C., Spirandelli, D., Franklin, E.C., Lynham, J., Kantar, M.B., Miles, W., Smith, C.Z., Freel, K., Moy, J., Louis, L.V., 2018. Broad threat to humanity from cumulative climate hazards intensified by greenhouse gas emissions. Nat. Clim. Chang. 8, 1062–1071.
Myeong, S., Nowak, D.J., Duggin, M.J., 2006. A temporal analysis of urban forest carbon storage using remote sensing. Remote Sens. Environ. 101, 277–282.
Myneni, R.B., Hall, F.G., Sellers, P.J., Marshak, A.L., 1995. The interpretation of spectral vegetation indexes. IEEE Trans. Geosci. Remote Sens. 33, 481–486.
Pecl, G.T., Araújo, M.B., Bell, J.D., Blanchard, J., Bonebrake, T.C., Chen, I.-C., Clark, T. D., Colwell, R.K., Danielsen, F., Evengård, B., 2017. Biodiversity redistribution under climate change: Impacts on ecosystems and human well-being. Science 355, eaai9214.
Perera, K., Saparamadu, M., Amarasinghe, M., 2011. Development of allometric equations to determine above and below ground biomass and organic carbon content in Bruguiera gymnorrhiza and Lumnitzera racemosa.
Rai, P., Vineeta, S., Manohar, G., Bhat, K.A., Kumar, J.A., Kumar, A., Cabral-Pinto, M., Chakravarty, M., 2021. Carbon storage of single tree and mixed tree dominant species stands in a reserve forest—Case study of the Eastern Sub-Himalayan Region of India. Land 10, 435.
Razali, S.M., Nuruddin, A.A., Lion, M., 2019. Mangrove vegetation health assessment based on remote sensing indices for Tanjung Piai, Malay Peninsular. J. Landscape Ecol. 12, 26–40.
Ruan, L., Yan, M., Zhang, L., Fan, X., Yang, H., 2022. Spatial-temporal NDVI pattern of global mangroves: A growing trend during 2000–2018. Sci. Total Environ. 844, 157075.
Shen, M., Kong, F., Tong, L., Luo, Y., Yin, S., Liu, C., Zhang, P., Wang, L., Chu, P.K., Ding, Y., 2022. Carbon capture and storage (CCS): Development path based on carbon neutrality and economic policy. Carbon Neutrality 1, 37.
Siikamäki, J., Sanchirico, J.N., Jardine, S.L., 2012. Global economic potential for reducing carbon dioxide emissions from mangrove loss. Proc. Natl. Acad. Sci. 109, 14369–14374.
Song, S., Ding, Y., Li, W., Meng, Y., Zhou, J., Gou, R., Zhang, C., Ye, S., Saintilan, N., Krauss, K.W., 2023. Mangrove reforestation provides greater blue carbon benefit than afforestation for mitigating global climate change. Nat. Commun. 14, 756.
Srivastava, P., Bal, S., 1984. Composition and distribution pattern of natural regeneration after second thinning in Matang Mangrove Reserves, Perak, Malaysia, Proceedings of the Asian Symposium on Mangrove Environment- Research and Management., pp. 761-784.
Su, X., Zhang, L., Meng, H., Wang, H., Zhao, J., Sun, X., Song, X., Zhang, X., Mao, L., 2024. Long-term conservation tillage increase cotton rhizosphere sequestration of soil organic carbon by changing specific microbial CO2 fixation pathways in coastal saline soil. J. Environ. Manage. 358, 120743.
Suardana, A.M.A.P., Anggraini, N., Nandika, M.R., Aziz, K., As-Syakur, A.R., Ulfa, A., Wijaya, A.D., Prasetio, W., Winarso, G., Dewanti, R., 2023. Estimation and mapping above-ground mangrove carbon stock using sentinel-2 data derived vegetation indices in Benoa Bay of Bali Province, Indonesia. Forest Soc. 7, 116–134.
Tang, L., Zhou, Q.S., Guo, W., Li, P., Gao, Y., 2021. Importance of high severity in a physical removal treatment for controlling invasive Spartina alterniflora. Ecol. Eng. 171, 106375.
Trujillo, L.P., Mancera-Pineda, J., Medina-Calderon, J., Zimmer, M., Schnetter, M., 2021. Massive loss of aboveground biomass and its effect on sediment organic carbon concentration: Less mangrove, more carbon? Estuarine Coastal Shelf Sci. 248, 106888.
Van Hespen, R., Hu, Z., Borsje, B., De Dominicis, M., Friess, D.A., Jevrejeva, S., Kleinhans, M.G., Maza, M., Van Bijsterveldt, C.E., Van der Stocken, T., 2023. Mangrove forests as a nature-based solution for coastal flood protection: Biophysical and ecological considerations. Water Sci. Eng. 16, 1–13.
Walcker, R., Gandois, L., Proisy, C., Corenblit, D., Mougin, É., Laplanche, C., Ray, R., Fromard, F., 2018. Control of “blue carbon” storage by mangrove ageing: Evidence from a 66-year chronosequence in French Guiana. Glob. Chang. Biol. 24, 2325–2338.
Wang, F., Liu, J., Qin, G., Zhang, J., Zhou, J., Wu, J., Zhang, L., Thapa, P., Sanders, C.J., Santos, I.R., 2023. Coastal blue carbon in China as a nature-based solution toward carbon neutrality. Innovation 4.
Warren, R., Price, J., VanDerWal, J., Cornelius, S., Sohl, H., 2018. The implications of the United Nations Paris Agreement on climate change for globally significant biodiversity areas. Clim. Change 147, 395–409.
Worthington, T.A., Spalding, M., Landis, E., Maxwell, T.L., Navarro, A., Smart, L.S., Murray, N.J., 2024. The distribution of global tidal marshes from earth observation data. Glob. Ecol. Biogeogr. 33, e13852.
Zhu, J.J., Yan, B., 2022. Blue carbon sink function and carbon neutrality potential of mangroves. Sci. Total Environ. 822, 153438.